SUPPLEMENTARY MATERIAL

METHODS

Masson's trichrome staining

For direct visualization of collagen fibres and histological assessment of collagen deposition, trichrome staining was performed using the Masson Trichrome Staining Kit (Sigma-Aldrich, St Louis, MO, USA).[1]

Hydroxyproline assay

Skin biopsies (3 mm) were placed in 6 M HCl for three hours at 120°C and the pH of the samples was adjusted to 7 with 6 M NaOH.[1] Samples were then mixed with 0.06 M chloramine T and incubated for 20 min at room temperature. 3.15 M perchloric acid and 20% p-dimethylaminobenzaldehyde were added and samples were incubated for additional 20 min at 60°C. The absorbance was determined at 557 nm with a Spectra MAX 190 micro plate spectrophotometer (Molecular Devices, Sunnyvale, California, USA).

Multiphoton microscopy

Multiphoton inverted stand Leica SP5 microscope (Leica Microsystems Gmbh, Wetzlar, Germany) was used for tissue imaging as previously described.[1-2] A Ti:Sapphire Chameleon Ultra (Coherent, Saclay, France) with a center wavelength at 810 nm was used as the laser source for generating second harmonic and two-photon excited fluorescence signals (TPEF).[3] The laser

beam was circularly polarized and equipped with a Leica Microsystems HCX IRAPO 25x/0.95 W objective was used to collect and excite second harmonic generation (SHG) and TPEF. Signals were detected in epi-collection through a 405/15-nm and a 525/50 bandpass filters respectively, by NDD PMT detectors (Leica Microsystems). LAS software (Leica, Germany) was used for laser scanning control and image acquisition.

Collagen SHG index

SHG and TPEF images were acquired using detectors with a constant voltage supply and constant laser excitation power allowing direct comparison of SHG intensity values. Analyses were performed using homemade Image J routine (http://imagej.nih.gov/ij/).[2,4] Two fixed thresholds were chosen to distinguish biological material from the background signal (TPEF images) and specific collagen fibers were imaged with SHG images. A score (collagen SHG score) was then established by comparing the area occupied by the collagen relative to the sample surface. TPEF (green) and SHG (red) images were pseudocoloured and overlaid for publication using Image J.

Murine model of excisional wound healing

Two 6 mm wounds, one on each side of the midline, were created on the shaved dorsa of mice. Digital photographs of the wounds were taken at 0, 7 and 14 days after wounding. Immediately prior to wound surgery mice were given either IVA337 at 30 mg/kg, IVA337 at 100 mg/kg, rosiglitazone at 5 mg/kg or vehicle by oral gavage. This daily regimen continued until the

wounds were harvested at 7 and 14 days and fixed in 10% wt/vol. buffered formalin. Macroscopic and microscopic wound analysis was performed as described previously.[5]

Isolation of primary fibroblasts and migration assay

Dermal fibroblasts were isolated from human skin by collagenase digestion as previously described.[6] Fibroblasts were cultured in DMEM supplemented with 10% fetal calf serum.

RTqPCR

Total RNA was isolated using RNeasy Mini Extraction Kit (Qiagen, Courtaboeuf, France). Gene expression assays were performed as previously described[6] with primer sequences obtained from Applied Biosystems (Courtaboeuf, France) for Col1A1 (Hs00164004-m1), Col1A2 (Hs00164099-m1) and α-SMA (Hs00426835-g1)[7]. Hypoxanthine phosphoribosyltransferase 1 (HPRT1) (Applied Biosystems, Hs99999909-m1) was used as a housekeeping control gene to normalize the amounts of cDNA within each sample. Differences were calculated using the Ct and comparative Ct methods for relative quantification. Results were expressed in arbitrary units, where Col1A1, Col1A2 and α-SMA genes were normalized with respect to HPRT1gene.

In PPARγ gene expression analysis RNA was isolated from cultured fibroblasts using RNeasy Mini Extraction Kit (Qiagen, Courtaboeuf, France). Contaminating genomic DNA was removed using a DNA-free kit (Ambion, Austin, USA). cDNA was synthesized from 1 µg RNA using iScript cDNA Synthesis kit from BioRad (Hercules, CA, USA). Custom made primers were supplied by Sigma-Aldrich (Saint-Quentin Fallavier, France) and used at 300nM.

Table 1. Primer sequences used in real-time qPCR

Gene	Forward primer	Reverse primer
HPPARgv1v2	GAATTAGATGACAGCGACTT	GTAGCAGGTTGTCTTGAATG
HPPARgv2	GCGATTCCTTCACTGATACACT	TGGAGTAGAAATGCTGGAGAAG
RPLP0	CTGATGGGCAAGAACACCAT	GTGAGGTCCTCCTTGGTGAA

Western blotting and cell fractionation

Protein was extracted from cultured fibroblasts using standard protein extraction protocols.[5,8] To separate nuclear and post nuclear fractions human fibroblasts were detached from plates using trypsin. Cell fractionation was performed using a nuclear extract kit purchased from Active Motif (La Hulpe, Belgium) and according to manufacturer's instructions. Whole cell lysate and nuclear fractions were subjected to SDS-PAGE separation and immunoblotting. Densitometry was performed on bands within the linear range and fold changes in levels calculated from this data as previously described.[8]

IVA337

IVA337 is a new patent protected chemical compound that activates all three PPAR isotypes: α, δ and γ. IVA337 is a pan PPAR agonist with the maximal effective concentration (EC_{50}) of 0.92 μM, 0.53 μM and 0.18 μM for human PPARα, PPARδ and PPARγ respectively. IVA337 was designed to produce moderate pan PPAR activation which translated into excellent safety profile

and absence of major side effects as demonstrated by the current trial. Mice were monitored for side effects and clinical signs including body weight, activity, posture, fur texture and skin integrity.

In the current mouse studies IVA337 was administered by gastrogavage at 30 mg/mL (batch IV0250033-01-35) and 100 mg/mL (batch IV0250033-01-35). IVA337 and rosiglitazone (5 mg/mL, batch IV0000199-01-10, B001550974) were formulated in 1% Methylcellulose (METOLOSE SM400, 400Cps) + 0.1% Poloxamer 188 as ready-to-use suspensions and stored at 5±3°C during the study. 1% Methylcellulose (METOLOSE SM400, 400Cps) + 0.1% Poloxamer 188 was used as vehicle and stored at 5±3°C during the study.

Antibodies and reagents

Antibodies specific for CD3 (ab5690), CD90 (ab181469), CD45 (ab10558), CD8 (ab22378), α-SMA (ab32575), nuclear matrix protein p84 (ab487), PPAR alpha (ab3484), PPAR delta (ab23673) PPAR gamma (ab19481) and isotype control IgG (ab171870) were purchased from Abcam (Cambridge, UK). Anti-Col1A1 (sc-8784) was purchased from Santa Cruz Biotechnology (Santa Cruz, CA, USA). Antibody for Smad2/3 (D7G7), phospho-Smad2/Smad3 (D27F4), phospho-p38 MAPK (D3F9), p38 MAPK (9212), phospho-p44/42 MAPK (Erk1/2) (Thr202/Tyr204), p44/42 MAPK (Erk1/2) (137F5) and inhibitor U0126 (9903) were purchased from Cell Signaling Technology (Leiden, The Netherlands). Anti-β-tubulin (T7816) was purchased from Sigma-Aldrich (Saint-Quentin Fallavier, France). Anti-CD107b (BD550292) and anti-Ly6G (BD 551459) were purchased from BD Biosciences (Le Pont de Claix, France). Anti-F4/80 (14-4801-85) was purchased from eBioscience (Paris, France). Human recombinant TGF-β1 antibodies were purchased from R&D Systems (Lille, France). Alexa-488- and Alexa-594-

tagged secondary antibodies were purchased from Molecular Probes (Invitrogen, Cergy Pontoise, France). Phalloidin DyLight 554 was purchased from Pierce Biotechnology (Rockford, IL, USA). SB431542 InSolution™ TGF-β RI Kinase Inhibitor VI and SB203580 p38 MAP kinase inhibitor were purchased from Merck Millipore (Darmstadt, Germany).

LEGENDS

Supplementary Figure 1. PPARα, PPARδ and PPARγ expression abnormalities in bleomycin-treated mouse skin are attenuated by IVA337. (A) Immunohistochemistry was performed on skin derived from mice treated with subcutaneous injection of NaCl or bleomycin. Scale bar is 50 μm. (B) Graphical representation PPARα, PPARδ and PPARγ expression in mouse skin harvested after 6 weeks of treatment with NaCl or bleomycin (n=5 per group). Bleo - denotes bleomycin; IVA337 (30 mg) denotes IVA337 at 30 mg/kg; IVA337 (100 mg) denotes IVA337 at 100 mg/kg. Four high power field images were captured and number of immune-positive cells was recorded. Bleomycin treatment was associated with significant decrease in PPARα and PPARγ expression and treatment with IVA337 at both low and high doses changed the expression of all three PPAR isoforms. *$p < 0.05$; **$p < 0.01$; ***$p < 0.001$

Supplementary Figure 2. Reduced fibrogenesis associated with IVA337 treatment in a model of fibrosis regression. (A) Representative images of H&E-stained sections of mouse skin treated with subcutaneous NaCl or bleomycin. Scale bar 100 μm. (B) Graphical representation of dermal thickness of mouse skin harvested after 6 weeks of NaCl or bleomycin. (N) denotes

NaCl; (B) denotes bleomycin; (30 mg) denotes IVA337 at 30 mg/kg; (100 mg) denotes IVA337 at 100 mg/kg; (rosi) denotes rosiglitazone at 5 mg/kg. Four high power field images were captured and two measurements per image were made. Results represent the relative fold change compared to NaCl-treated control mice. (C) Representative images of Masson's Trichrome-stained sections of mouse skin harvested after 6 weeks of treatment with NaCl or bleomycin. Scale bar 100 μm. (D) Graphical representation of hydroxyproline assay. Results are represented as means ±SEM of triplicate measurements obtained from n = 6 mice (2 biopsies per mouse) and shown as relative fold change compared to NaCl-treated control samples. (E) Representative images of α-SMA immunohistochemistry. Scale bar 50 μm. (F) Graphical representation of relative number of α-SMA-positive cells in dermis of NaCl or bleomycin-treated mice.

Supplementary Figure 3. Quantitative analysis of SHG images in histological sections of mouse skin. Simultaneous TPEF/SHG acquisition using circular polarization and SHG signals were selectively processed to obtain a binary distribution of SHG after applying a threshold. TPEF images (green) and SHG (red) images were pseudocoloured and overlaid (yellow). (A) Representative TPEF/SHG collagen images of mouse skin treated with bleomycin for 21 days in (A) and 42 days in (B). Note morphological changes in collagen fibril (yellow) length, thickness, alignment and density in NaCl and bleomycin treated skin in (A) preventative and (B) curative trials. Reduced collagen density (yellow) is evident in IVA337 treated dermis compared to vehicle controls. All images were acquired using 25× 0.95 water objective lens. Excitation wavelength is at 810 nm. Collagen SHG signal was collected using a 405/15-nm and 525/50 band-pass filters. Scale bar 50μm. (C) Quantitative collagen analysis based on collagen SHG images. Note that all images were acquired with the same excitation power, and the intensities

are directly comparable. All values represent means ±SEM; n = 5 each group. *p < 0.05; **p < 0.01; ***p < 0.001

Supplementary Figure 4. Effect of IVA337 treatment on PPARγ1 and PPARγ2 mRNA expression in cultured fibroblasts. (A) SSc fibroblasts were treated with TGF-β1 (10 ng/ml) and IVA337 (10 μM) for 24 hours (n=6). Treatment with TGF-β1 (10 ng/ml) significantly decreased PPARγ1, but not PPARγ2 mRNA level. Pre-incubation with IVA337 (10 μM) in TGF-β-treated fibroblasts caused a significant increase in PPARγ1 gene expression. Differences were calculated using the Ct and comparative Ct methods for relative quantification. Results were expressed in arbitrary units, where PPARγ1 and PPARγ2 genes were normalized with respect to RPLPO housekeeping gene. All values represent means and ±SEM; n = 6 each group. *p < 0.05

Supplementary Figure 5. Despite of having anti-fibrotic effects IVA337 does not impair wound healing. (A) Representative digital images of full-thickness excisional wounds on the backs of mice treated with vehicle, IVA337 (30 and 100 mg/kg) and rosiglitazone at 5 mg/kg for 7 and 14 days. (B) Graphical representation of wound diameter and (C) surface wound area at 0, 7 and 14 days after surgery. All values represent means and ±SEM; n=6 mice, 12 wounds each group/time point.

Supplementary Figure 6. Expression of PPARδ protein in wounded mouse skin. (A) Representative immunohistochemistry images of mouse skin staining for PPARδ protein 7 and 14 days after wounding. Vehicle, IVA337 (30 mg/kg) or rosiglitazone (5 mg/kg) were administered by gastrogavage every second day until the end point. PPARδ is expressed in the epidermis and dermis. IVA337-treated mice showed significantly higher levels of PPARδ compared to vehicle controls at both time points. PPARδ expression is downregulated at day 14 compared to day 7 IVA337-treated wounds. Scale bar 50 μm. (B) Quantification of PPARδ immune-positive cells. Four high power field images were captured and number of PPARδ-positive cells was recorded. n = 5 each group. *$p < 0.05$; **$p < 0.01$

REFERENCES

1 Ruzehaji, N. et al. Combined effect of genetic background and gender in a mouse model of bleomycin-induced skin fibrosis. Arthritis research & therapy **17**, 145, doi:10.1186/s13075-015-0659-5 (2015).

2 Gailhouste, L. et al. Fibrillar collagen scoring by second harmonic microscopy: a new tool in the assessment of liver fibrosis. Journal of hepatology **52**, 398-406, doi:10.1016/j.jhep.2009.12.009 (2010).

3 Chen, X., Nadiarynkh, O., Plotnikov, S. & Campagnola, P. J. Second harmonic generation microscopy for quantitative analysis of collagen fibrillar structure. Nature protocols **7**, 654-669, doi:10.1038/nprot.2012.009 (2012).

4 Guilbert, T. et al. A robust collagen scoring method for human liver fibrosis by second harmonic microscopy. Optics express **18**, 25794-25807, doi:10.1364/OE.18.025794 (2010).

5 Ruzehaji, N. et al. Attenuation of flightless I improves wound healing and enhances angiogenesis in a murine model of type 1 diabetes. Diabetologia **57**, 402-412, doi:10.1007/s00125-013-3107-6 (2014).

6 Wipff, J. et al. Dermal tissue and cellular expression of fibrillin-1 in diffuse cutaneous systemic sclerosis. Rheumatology **49**, 657-661, doi:10.1093/rheumatology/kep433 (2010).

7 Avouac, J. et al. Angiogenesis in systemic sclerosis: impaired expression of vascular endothelial growth factor receptor 1 in endothelial progenitor-derived cells under hypoxic conditions. Arthritis and rheumatism **58**, 3550-3561, doi:10.1002/art.23968 (2008).

8 Lei, N. et al. Flightless, secreted through a late endosome/lysosome pathway, binds LPS and dampens cytokine secretion. Journal of cell science **125**, 4288-4296, doi:10.1242/jcs.099507 (2012).

Supplementary Figure 1.

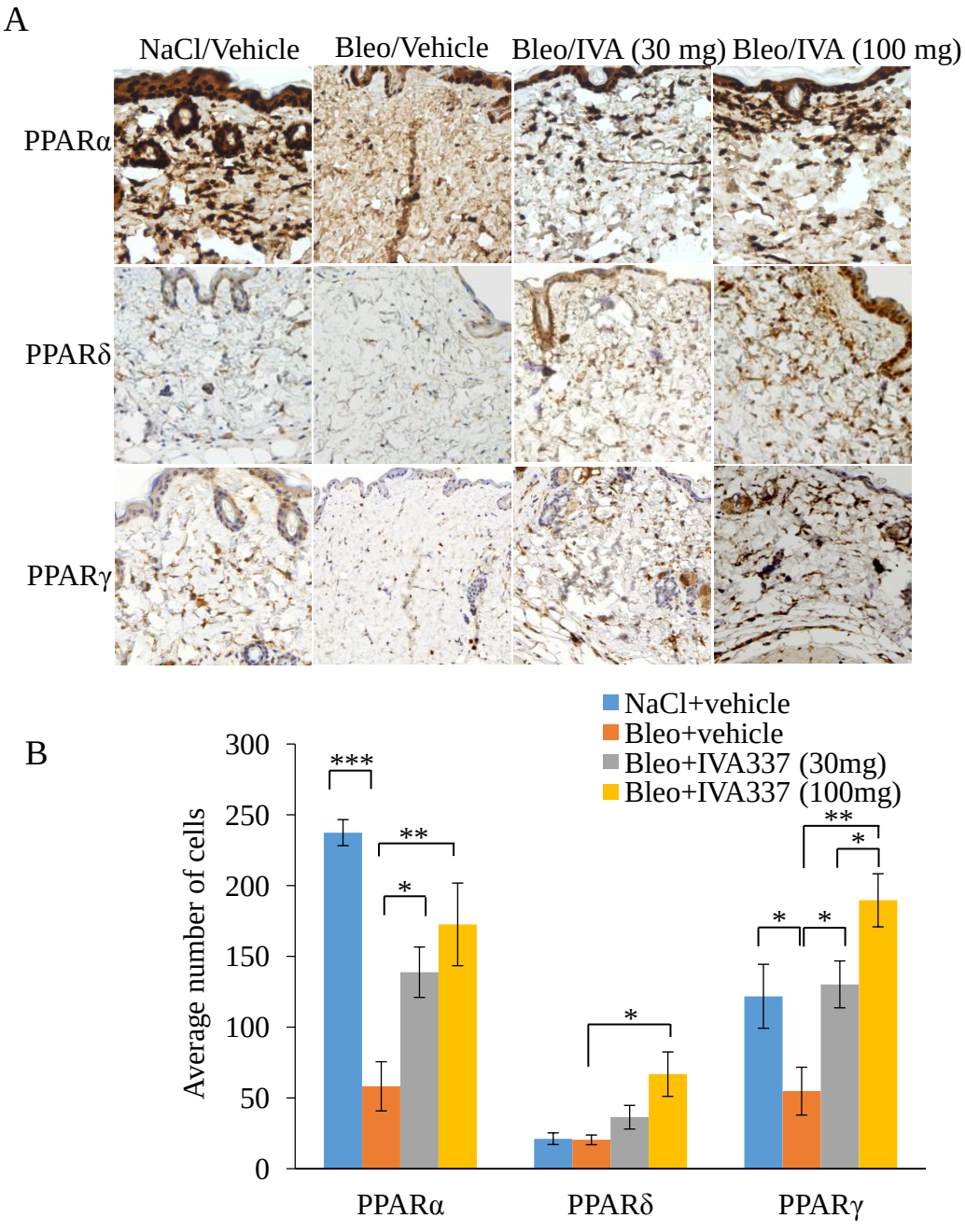

Supplementary Figure 2.

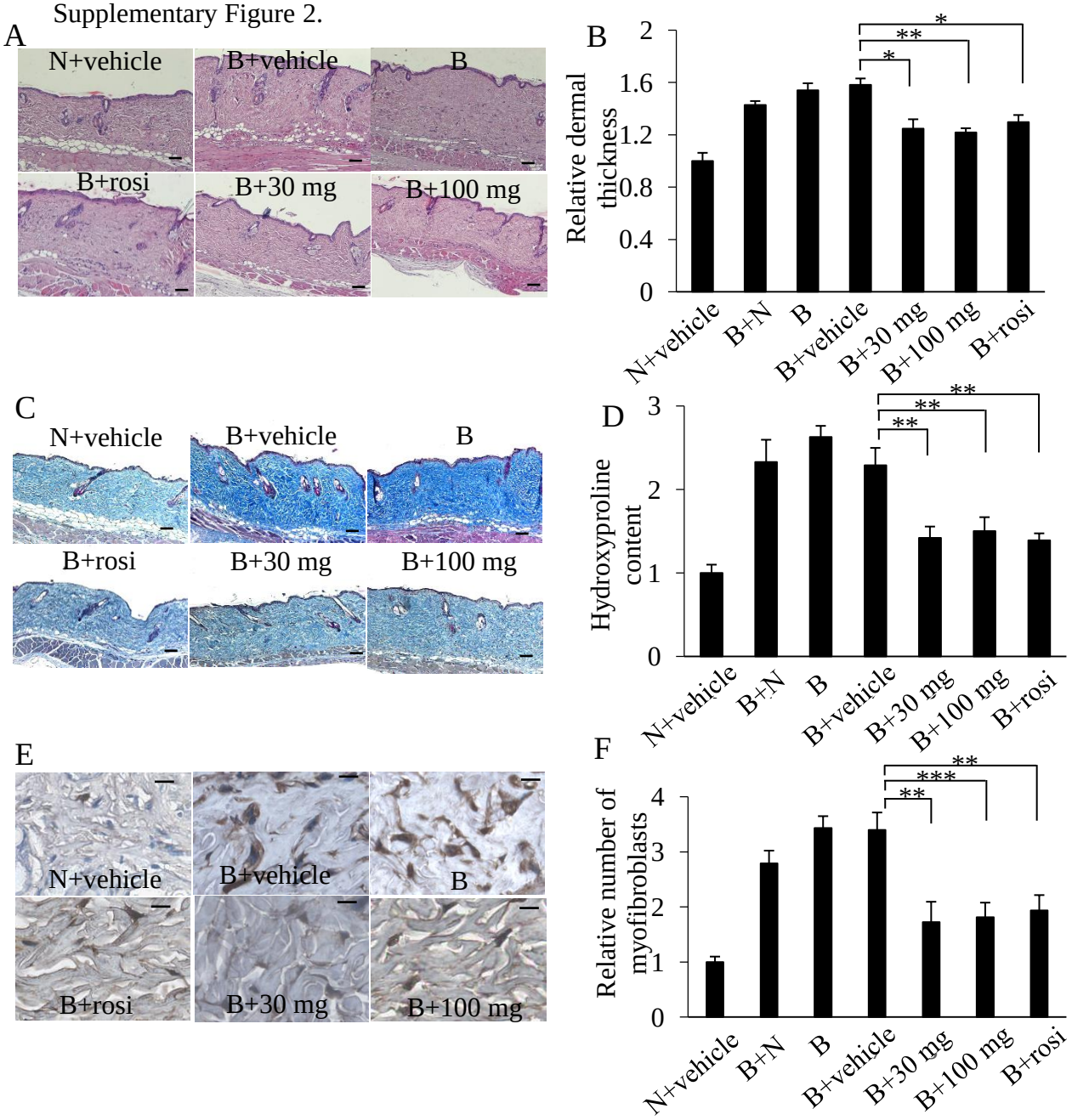

Supplementary Figure 3.

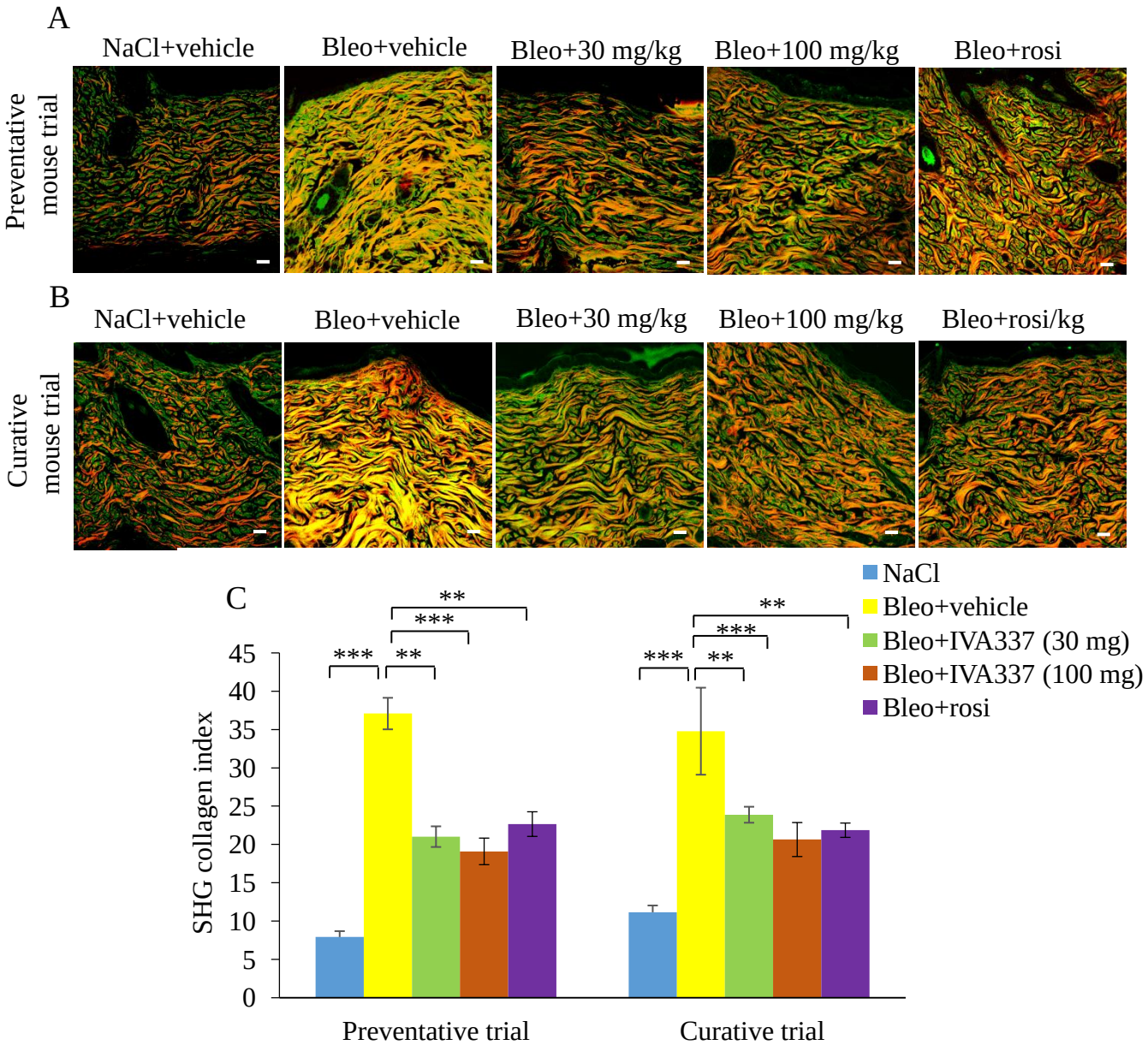

Supplementary Figure 4.

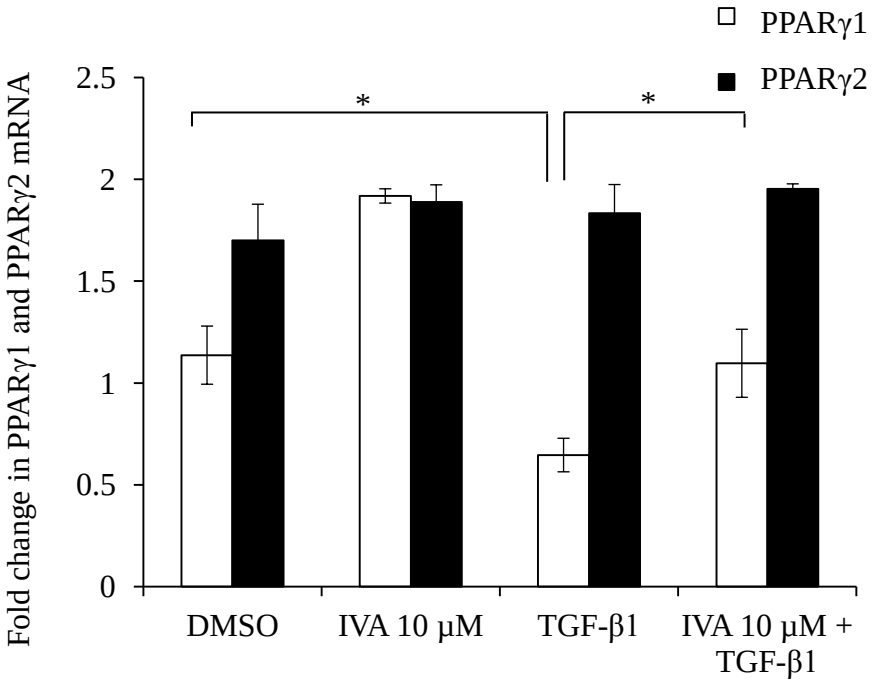

Supplementary Figure 5.

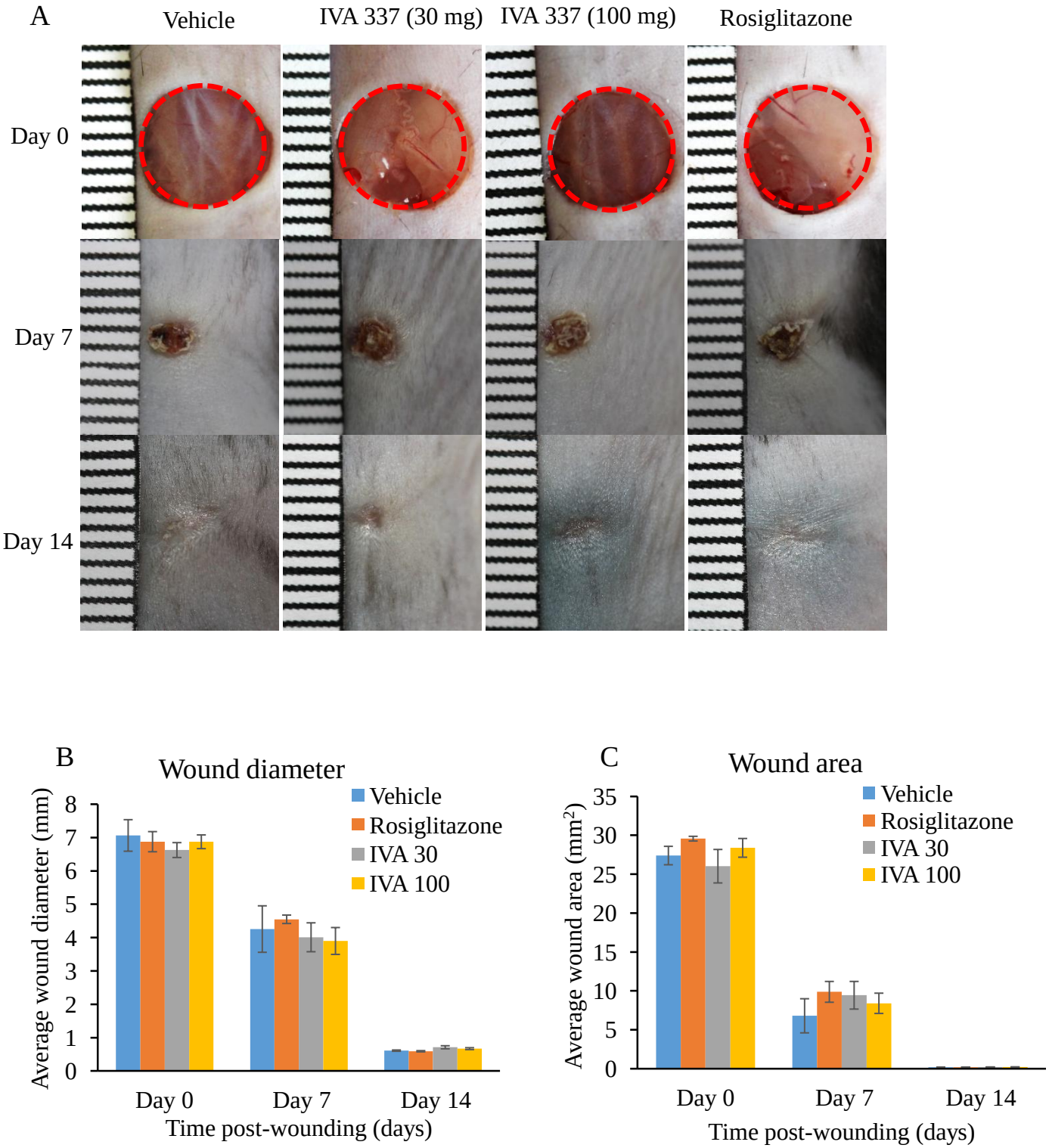

Supplementary Figure 6.